Targeting of incoming retroviral Gag to the centrosome involves a direct interaction with the dynein light chain 8

Coralie Petit[1], Marie-Lou Giron[1], Joelle Tobaly-Tapiero[1], Patricia Bittoun[1], Eléonore Real[2], Yves Jacob[2], Noël Tordo[2], Hugues de Thé[1] and Ali Saïb[1,*]

[1]CNRS UPR9051, Hôpital Saint-Louis, Conventionné par l'Université Paris 7, 1 avenue Claude Vellefaux, 75475 Paris Cedex 10, France
[2]Laboratoire des Lyssavirus, Institut Pasteur, 25 rue du Dr Roux, 75724 Paris Cedex 15, France
*Author for correspondence (e-mail: alisaib@infobiogen.fr)

Accepted 14 April 2003
Journal of Cell Science 116, 3433-3442 © 2003 The Company of Biologists Ltd
doi:10.1242/jcs.00613

Summary

The role of cellular proteins in the replication of retroviruses, especially during virus assembly, has been partly unraveled by recent studies. Paradoxically, little is known about the route taken by retroviruses to reach the nucleus at the early stages of infection. To get insight into this stage of virus replication, we have studied the trafficking of foamy retroviruses and have previously shown that incoming viral proteins reach the microtubule organizing center (MTOC) prior to nuclear translocation of the viral genome. Here, we show that incoming viruses concentrate around the MTOC as free and structured capsids. Interestingly, the Gag protein, the scaffold component of viral capsids, targets the pericentrosomal region in transfected cells in the absence of any other viral components but in a microtubule- and dynein/dynactin-dependent manner. Trafficking of Gag towards the centrosome requires a minimal 30 amino acid coiled-coil motif in the N-terminus of the molecule. Finally, we describe a direct interaction between Gag and dynein light chain 8 that probably accounts for the specific routing of the incoming capsids to the centrosome prior to nuclear import of the viral genome.

Key words: Retrovirus, Cytoskeleton, Trafficking, Spumavirus

Introduction

After penetration into the host cell, pathogens have to reach their sites of replication. To facilitate their spread within the infected cells, viruses have evolved many specific mechanisms to hijack the cellular cytoskeleton (Ploubidou and Way, 2001). For example, microtubules (MTs) are essential for the herpes simplex virus (HSV) (Sodeik et al., 1997), adenovirus (Suomalainen et al., 1999) and vaccinia virus (VV) (Ploubidou et al., 2000) to reach the nuclei of the infected cells. VV is unique because it sequentially exploits the MT network for its intracellular movement (Rietdorf et al., 2001; Ward and Moss, 2001) and the actin cytoskeleton to enhance its cell-to-cell spread (Geada et al., 2001; Hollinshead et al., 2001). Intracellular VV particles are propelled on actin tails those formation is induced by the virus itself, which mimics the cellular receptor tyrosine kinase signaling cascades that normally occur for actin polymerization at the plasma membrane (Frischknecht et al., 1999; Frischknecht and Way, 2001; Moreau et al., 2000), a situation already reported for intracellular movements of *Listeria* and *Shigella* (reviewed in Frischknecht and Way, 2001). In the case of the murine leukemia virus (MuLV), an interaction between the Gag protein, the scaffold component of retroviral capsids, and KIF4, a microtubule plus-end directed motor, is needed for trafficking towards the plasma membrane during the late step of infection (Tang et al., 1999). However, despite our growing knowledge of host-virus interactions, little is known about how retroviruses are transported from the periphery to the center of the cell during the early stages of infection. Gaining better insight into the mechanism by which retroviruses move within the infected cells might improve retrovirus-based gene therapy and might allow the design of new therapeutic approaches against retroviral pathogens.

Spumaviruses, also known as foamy viruses (FVs), are complex animal retroviruses that encode structural (Gag, Env), enzymatic (Pol) and regulatory products (Tas, Bet). Although surface Env glycoproteins are needed to enter target cells, interaction and subsequent self-multimerization of Gag molecules lead to capsid formation (Eastman and Linial, 2001; Tobaly-Tapiero et al., 2001). Several functional regions were identified along the scaffold Gag protein. There are three glycine(G)/arginine(R)-rich sequences, the so-called GR boxes, in the C-terminus that are implicated in viral nucleic acid binding and harbor a nuclear localization sequence (NLS) (Schliephake and Rethwilm, 1994; Yu et al., 1996), a 18 amino acid motif (amino acids 43-60) resembling the cytoplasmic targeting and retention signal (CTRS) of type D retroviruses that allows cytoplasmic targeting of Gag (Eastman and Linial, 2001) and, finally, a coiled-coil domain (amino acids 130-160) that is necessary for Gag-Gag interaction (Tobaly-Tapiero et al., 2001). The last two motifs are required for capsid assembly. Although compelling studies have demonstrated the requirement for Gag in the late steps of infection (i.e.

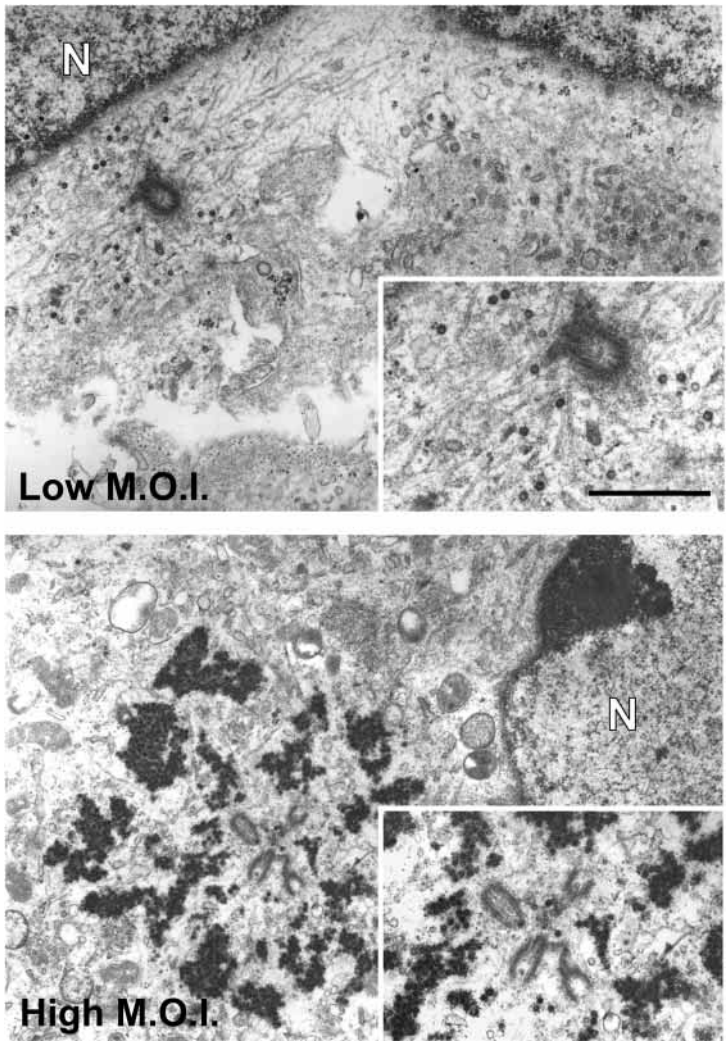

Fig. 1. MTOC targeting of incoming HFV in the early step of infection. Five hours after infection, numerous free incoming viral capsids are detected around the centrosome at a low (top) and a high (bottom) m.o.i. by electron microscopy. Viral capsids in close vicinity to microtubules are easily observed in the higher resolution picture of the centrosomal region. Scale bar, 450 nm (upper and lower insets). N, nucleus.

packaging of genomic RNA or virus egress), little is known about its role during the early steps of virus cycle.

We have previously shown that incoming human foamy virus (HFV), the prototype of FVs, targets the microtubule organizing center (MTOC) prior to nuclear translocation. Centrosomal targeting of incoming viral proteins and subsequent viral replication were inhibited by a treatment with nocodazole, demonstrating the involvement of the MT network in FV replication (Saib et al., 1997). However, the precise status of the viral material at the MTOC and the mechanism of transport towards this organelle were unknown. Here, we show that incoming HFV reaches the MTOC as naked and structured capsids. Remarkably, the Gag protein by itself harbors the determinant to target the MTOC, requiring a domain of 30 amino acids predicted to fold into a coiled coil. Transport of Gag to the MTOC necessitates the retrograde, MT-dependent, dynein/dynactin motor because it is prevented by overexpression of the central coiled-coil domain (CC1) of p150^{Glued}, the dynactin sidearm subunit. Finally, a direct interaction between HFV Gag and the cytoplasmic light chain of the dynein LC8 was described, identifying a molecular basis of retroviral transport in infected cells during the early steps of infection.

Materials and Methods

Recombinant DNA

All HFV sequences were initially derived from pHFV13, the infectious clone of HFV. Gag expression plasmids were generated by insertion of the 2.54 kb *Bsu*36I (full-length Gag, pSG-Gag) and 1.77 kb *Avr*II (pSG-Gag575) fragments into the *Sma*I site of the eukaryotic expression vector pSG5M as already described (Tobaly-Tapiero et al., 2001). The full-length green fluorescent protein (GFP)-Gag expression plasmid (pGFP-Gag) was generated by inserting the PCR product of the Gag open reading frame into the *Bam*HI/*Hin*dIII sites of pEGFP-C1 (Clontech). Mutants M1 to M8 (except M7) were derived from the pGFP-Gag plasmid following either digestion with appropriate restriction enzymes or by the QuickChange Mutagenesis kit (Stratagene). The sequence encoding the first 200 amino acids of Gag was amplified by PCR and inserted into the *Eco*RI-*Bam*HI sites of the pEGFPN1 vector (Clontech), leading to the M7 mutant. The infectious clone harboring the L171G mutation in the Gag open reading frame (ORF) was obtained by subcloning the 2884 bp *Eag*I-*Swa*I fragment of pHFV13 (generated by PCR) into the pGEM-T vector (Promega). Following site-directed mutagenesis, the *Eag*I-*Swa*I fragment harboring the GagL171G mutation was re-inserted into pHFV13 at the corresponding restriction sites, producing pHFVGagL171G. The pCgp9 vector encoding for HFV Gag and Pol proteins was kindly provided by Axel Rethwilm. The DsRed-CC1 expression vector was kindly provided by T. Schroer. GFP-LC8 has been generated by inserting a PCR-amplified LC8 cDNA (the hDLC1 isoform) into pEGFP-C1 (Clontech) at the *Bam*HI site. LC8$_{Flag}$ was already described (Jacob et al., 2000). Primers used in PCR amplification, or mutagenesis, are available on request.

Cell culture and transfection

Hamster BHK21 and simian Cos6 cells were maintained in DMEM (Gibco) supplemented with 5% fetal calf serum, 100 μg ml^{-1} penicillin, 50 μg ml^{-1} streptomycin, 2 mM glutamine and 240 mM Hepes. For transfection assays, 2×10^5 Cos6 cells were transfected with 2 μg recombinant plasmid DNA with the Lipofectin reagent (Gibco BRL) as specified by the manufacturer. 20 hours after transfection, cells were fixed and permeabilized with methanol at –20°C for 5 minutes. HFV Gag was detected by rabbit polyclonal anti-Gag antibodies (1/400 dilution). Monoclonal antibodies (mAbs) against vimentin (clone V18, used at 1/100 dilution; Sigma) and antibodies directed against a centriolar component (provided by M. Bornens, Curie Institute; clone CTR910, used at 1/100 dilution) were used in some experiments. Fluorescein (FITC) or Texas red (TR)-coupled antibodies were used as second fluorescent conjugates (Biosys, dilution 1/800 in PBS-Tween 0.1%). Cells nuclei were stained with DAPI.

For confocal analysis, cells were mounted in Mowiol (Calbiochem) and examined using a BioRad MRC-1024 confocal imaging system (BioRad Microscience) and an inverted Diaphot 300 Nikon microscope. For fluorescein, a krypton/argon laser (Ion Laser Technology) with a 488 nm filter was used. For TR staining, an ion laser with a 568 nm filter was used. Images of FITC, TR and DAPI were pseudocolored in green, red and blue, respectively.

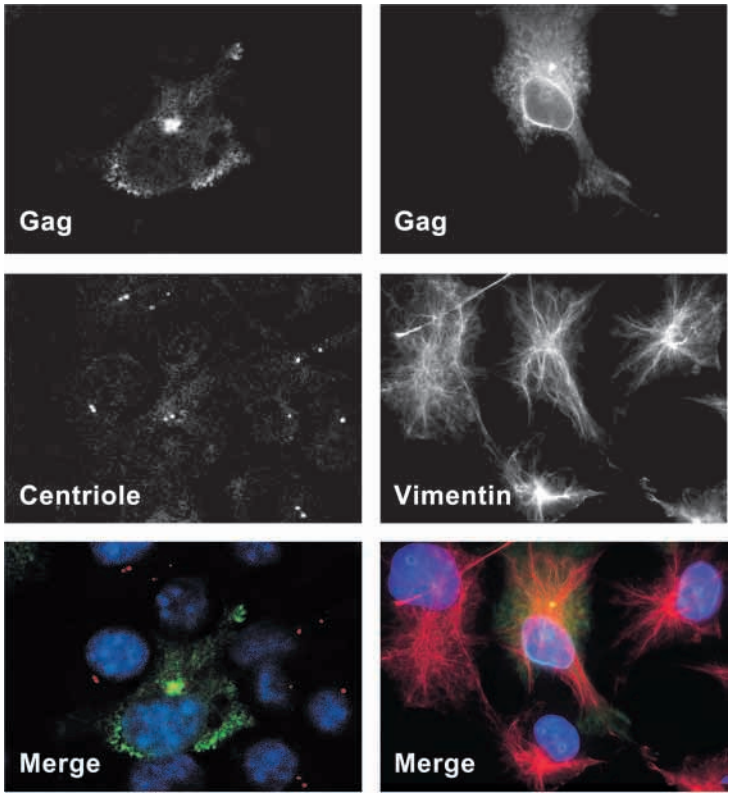

Fig. 2. The structural Gag protein targets the MTOC in transfected Cos6 cells. Following transfection of the full-length Gag expression vector, a confocal section reveals that HFV Gag proteins are mainly detected around the MTOC, which is revealed by the CTR910 antibody (left). In Gag-expressing cells, the vimentin network is not affected as observed by fluorescence microscopy (right). Nuclei are stained with DAPI.

Virus titers were determined using indicator FV-activated GFP expression (FAG) cells, which harbor the GFP ORF under the control of the HFV long terminal repeat (LTR), as previously described (Tobaly-Tapiero et al., 2001). Thus, the titers were measured as fluorescent cell-forming-units (FCFU) per ml.

Protein analysis

24 hours after transfection with pSG-Gag$_{575}$, pSG-Gag$_{575}$L171G or pLC8$_{Flag}$, or co-transfection of these vectors, 293T cells were labeled with [^{35}S]methionine-cysteine (200 μCi ml^{-1}, 1.175 Ci mmol^{-1} specific activity, Dupont NEN) for 3 hours. Cells were rinsed with cold PBS and then lysed with 10 mM Tris-HCl (pH 7.5), 50 mM NaCl, 1 mM $CaCl_2$, 3 mM $MgCl_2$ and anti-protease cocktail (Sigma), followed by centrifugation at 20,000 ***g*** for 5 minutes at 4°C. Cytoplasmic proteins were directly analysed by western blot using rabbit anti-Gag antibodies following denaturation in Laemmli buffer or immunoprecipitated with anti-Flag M2 mAb (Sigma) in CHAPS buffer (10 mM Tris pH 7.5, 150 mM NaCl, 1% CHAPS, 1 mM PMSF). For that purpose, pre-cleared cell extracts were incubated overnight at 4°C with the M2 anti-Flag mAb in CHAPS buffer, absorbed in protein-A/Sepharose. Immune complexes were centrifuged and washed four times in CHAPS buffer and analysed by western blot using anti-Gag antibodies (1/100). For western-blot analyses, proteins were resolved using SDS 10% polyacrylamide gel electrophoresis.

Culture supernatants of Cos6 cells transfected with pHFV13, pHFVGagL171G or a plasmid encoding only the Gag and Pol proteins (pCgp9; kindly provided by A. Rethwilm) were first cleared from cellular debris and then centrifuged through a 20% sucrose cushion in a solution containing 100 mM NaCl, 10 mM Tris-HCl (pH 7.4), and 1 mM EDTA at 80,000 ***g*** for 3 hours in a SW41 rotor at 4°C. The resulting pellets (containing the extracellular viruses) and cellular viral protein extracts from the parental cells were visualized by immunoblotting with rabbit anti-Gag antibodies (1/100) and peroxidase-conjugated antibodies, and revealed by enhanced chemiluminescence (Amersham). GFP-Gag fusions were analyzed by western blot using a polyclonal anti-GFP antibody (sc-8334, TEBU, 1/100). Prediction of the coiled-coil motifs was performed with the COILS program (http://www.ch.embnet.org/software/COILS_form.html).

Electron microscopy

Monolayers were fixed in situ with 1.6% glutaraldehyde (Taab Laboratory Equipment, Reading, UK) in 0.1 M Sörensen phosphate buffer, pH 7.3-7.4 for 1 hour at 4°C. Cells were scraped from their plastic substratum and centrifuged. The resulting pellets were successively post-fixed with 2% aqueous osmium tetroxide for 1 hour at room temperature, dehydrated in ethanol and embedded in Epon. Ultrathin sections were collected on 200-mesh copper grids coated with Formvar and carbon, and stained with uranyl acetate and lead citrate prior to observation with a Philips 400 transmission electron microscope, at 80 kV, at 2800-36,000 × magnification.

Results

HFV Gag targets the centrosome of transfected cells

We have previously shown that, prior to nuclear import, incoming HFV Gag proteins concentrate around the MTOC (Saib et al., 1997). This targeting and subsequent virus production were prevented by treating the cells with nocodazole, reflecting the importance of MTs in viral replication. Moreover, we reported that, as early as 5 hours after infection, most of incoming Gag antigens concentrated around the MTOC (Saib et al., 1997). However, it was unknown whether Gag is transported to the centrosome as free assembled capsids or as unstructured aggregates (as is the case for other retroviruses; McDonald et al., 2002). To deal with this issue, permissive BHK21 cells were infected with HFV at a low (1) and a high (10) multiplicity of infection (m.o.i.), fixed 5 hours later and analysed by electron microscopy (EM). As shown in Fig. 1, incoming viruses were mainly detected as naked and intact capsids of ~50 nm diameter near the MTOC, close to MTs. Analysis of a dozen EM thin sections of infected cells revealed an average of 20 capsids per section around the MTOC at low m.o.i. and an average of 600 capsids per section at high m.o.i. Viral capsids were never observed in the nucleus or close to nuclear pores.

Because Gag is the main component of capsids, we next assessed whether Gag by itself, in the absence of the viral genome and other viral proteins, could still reach the centrosome. For that purpose, a full-length Gag expression vector (pSG-Gag) was transfected into Cos6 cells and Gag localization was followed by confocal microscopy using polyclonal anti-Gag antibodies. 20 hours after transfection, Gag was mainly detected as a unique cytoplasmic dot, close to the nucleus (Fig. 2, left). Double labeling using a mAb (clone CTR910) directed against a centriolar component confirmed that this staining corresponds to the accumulation of Gag

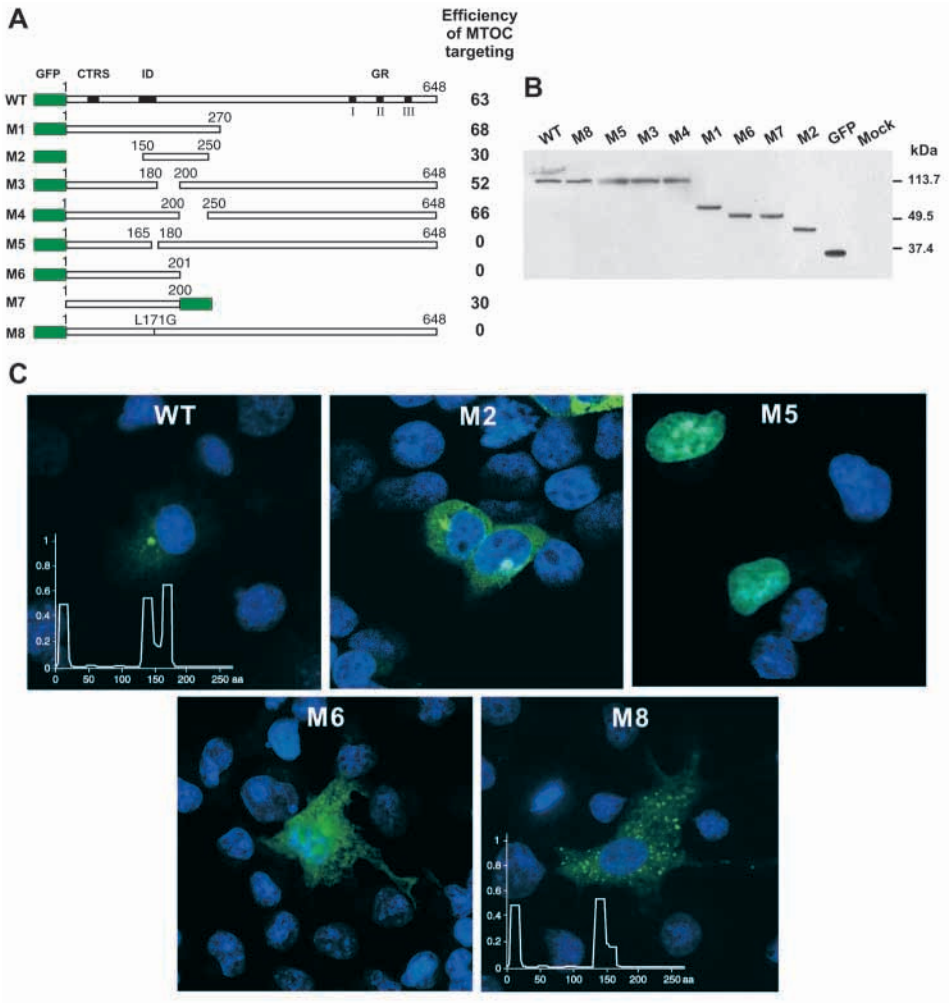

Fig. 3. (A) Minimal Gag sequence requirement for MTOC targeting. Schematic representation of the GFP-Gag fusion proteins. The locations of the three glycine/arginine rich motifs (GR I, II, III), the Gag-Gag interaction domain (ID) and the cytoplasmic targeting and retention signal (CTRS) are indicated by black boxes. The numbers indicate the percentage of GFP-positive cells harboring a centrosomal staining; values are the average of three independent experiments. (B) Western-blot analysis of the different GFP fusions revealed by rabbit anti-GFP antibodies. (C) Subcellular localization of GFP-Gag fusions as observed by fluorescence microscopy and prediction of coiled-coil motifs in the first 270 amino acids of HFV Gag as revealed by the COILS program (matrix: MTIDK, weight of 2.5 for position N).

molecules around the centrosome (Fig. 2, left). Expression of other structural (Pol and Env) or regulatory (Tas and Bet) viral proteins never leads to a centrosomal staining (data not shown).

It has been recently shown that cytoplasm-replicating large DNA viruses such as poxviruses and African swine fever virus (ASFV), assemble in aggresomes (Heath et al., 2001), a structure located close to the MTOC and generated in response to high levels of misfolded proteins (Johnston et al., 1998; Kopito, 2000). Aggresome formation induces a striking redistribution of the intermediate filament protein vimentin into a characteristic halo-like cage around aggregates of proteins (Kopito, 2000). To determine whether accumulation of Gag around the MTOC corresponded to the formation of an aggresome owing to a high level of Gag expression in transfected cells, Cos6 cells transfected with pSG-Gag were labeled with both anti-Gag and anti-vimentin antibodies. As shown by fluorescence microscopy (Fig. 2, right), the vimentin network is not affected in Gag-expressing cells, demonstrating that accumulation of Gag around the MTOC does not lead to the formation of an aggresome.

Mapping of the minimal Gag sequence involved in MTOC targeting

Several functional domains have been already mapped along the HFV Gag protein. To determine whether these domains (the C-terminal GR boxes and the two recently characterized N-terminal regions responsible for Gag self-assembly) are involved in MTOC targeting, the subcellular localization of a full-length GFP-Gag fusion protein and of deletion mutants was investigated (Fig. 3A). Cos6 cells were transfected with these constructs and the GFP fluorescence was directly observed 20 hours after transfection, following cell fixation. Although GFP alone diffusely localizes in both the cytoplasm and the nucleus of transfected cells, and never accumulates around the MTOC (data not shown), fusion of GFP to the full-length Gag targets the fusion protein to the centrosome (Fig. 3C). Serial deletions of the C-terminus of Gag, up to residue 270 (mutant M1), do not impair MTOC targeting of the corresponding GFP-Gag fusions. Deletion of amino acids 180-200 (mutant M3) or 200-250 (mutant M4) has no effect on MTOC targeting, whereas deletion of amino acids 165-180 (mutant M5) totally abolishes centrosomal targeting. Finally, GFP-Gag150-250 (mutant M2) is present around this organelle. Taken together, these results suggest that the domain implicated in MTOC targeting encompasses amino acids 150-180. This conclusion is, however, clouded by the fact that the M6 mutant encoding for GFP-Gag1-201 is no longer detected at the centrosome. To assess whether the absence of MTOC targeting of mutant M6 is due to inadequate positioning of the putative implicated

domain regarding the entire fusion protein, the first 200 amino acids of Gag were fused to the N-terminus of GFP and transfected in Cos6 cells. In that case, the fusion protein Gag1-200-GFP (mutant M7) was detected at the centrosome, suggesting that the domain involved in MTOC targeting must be flanked with minimal amino acid sequences at both sides to be functional. Taken together, these results indicate that proper centrosomal targeting does not require the presence of the GR boxes or the domains involved in capsid assembly, but necessitates the sequence between amino acids 150 and 180. All constructions were controlled by sequence analysis and protein expression was verified by western blot (Fig. 3B).

It is noteworthy that the N-terminus of HFV Gag harbors three putative coiled-coil motifs as revealed by the COILS program (Tobaly-Tapiero et al., 2001). We have previously shown that the coiled-coil motif located between amino acids 130 and 160 is crucial for Gag-Gag interaction (Tobaly-Tapiero et al., 2001). Interestingly, the second coiled-coil encompassing amino acids 160-180 strikingly matches the domain required in MTOC targeting identified here. To assess whether this motif is involved in centriolar targeting, we have generated a GFP-Gag fusion harboring a mutation at position 171 exchanging a crucial leucine into a glycine, disrupting the coiled-coil motif (mutant M8). As shown in Fig. 3C, this mutant is no longer able to reach the centrosome in transfected Cos6 cells.

Dynein-dynactin is required for centrosomal targeting of Gag

Retrograde movements along the MTs (minus-end-directed MT transport) require the dynein motor complex, which is assisted by the 20S dynactin cofactor (Karki and Holzbaur, 1999). The motor activity can be dislodged from the cargo by overexpression of p50/dynamitin, a component of the dynactin complex, disrupting their association (Burkhardt et al., 1997). This approach is widely used to demonstrate the involvement of the dynein-dynactin complex in the movement of viruses (Alonso et al., 2001; Dohner et al., 2002; Sodeik et al., 1997; Suomalainen et al., 1999). However, whereas dynamitin overexpression was reported to have no other effect on the cytoskeleton in HeLa cells (Burkhardt et al., 1997), it might affect MT organization and centrosome integrity in Cos cells (Quintyne et al., 1999). Interestingly, it has been shown that overexpression of the central coiled-coil domain (CC1) of p150^{Glued}, the dynactin sidearm subunit, has a more specific inhibitory effect on dynein-based transport than does p50/dynamitin (Quintyne et al., 1999). Thus, in our assays, HeLa cells and a CC1-expressing vector were used instead of Cos6 cells and p50/dynamitin. As shown in Fig. 4A, overexpression of DsRed-CC1 did not affect the MT network, confirming previous studies. However, the presence of CC1 prevented MTOC targeting of Gag in co-transfected HeLa

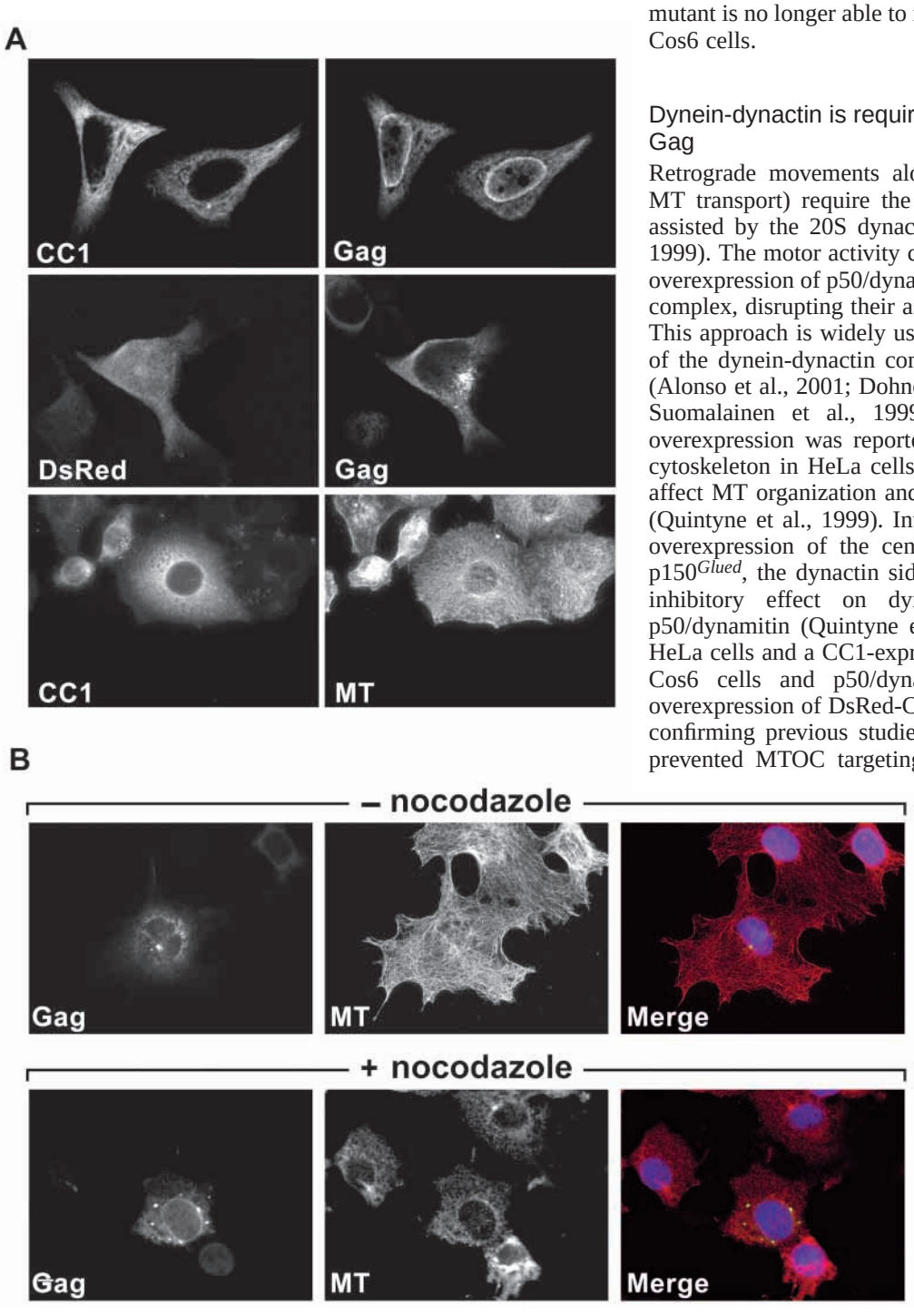

Fig. 4. (A) Involvement of the dynein-dynactin complex in MTOC targeting of Gag. In cells overexpressing CC1, the central coiled-coil domain of p150^{Glued}, GFP-Gag is no longer able to reach the centrosome (top). By contrast, expression of CC1 does not disrupt the MT network (bottom). (B) Following nocodazole treatment, GFP-Gag is no longer linked to the pericentrosomal region but dispersed within the cytoplasm.

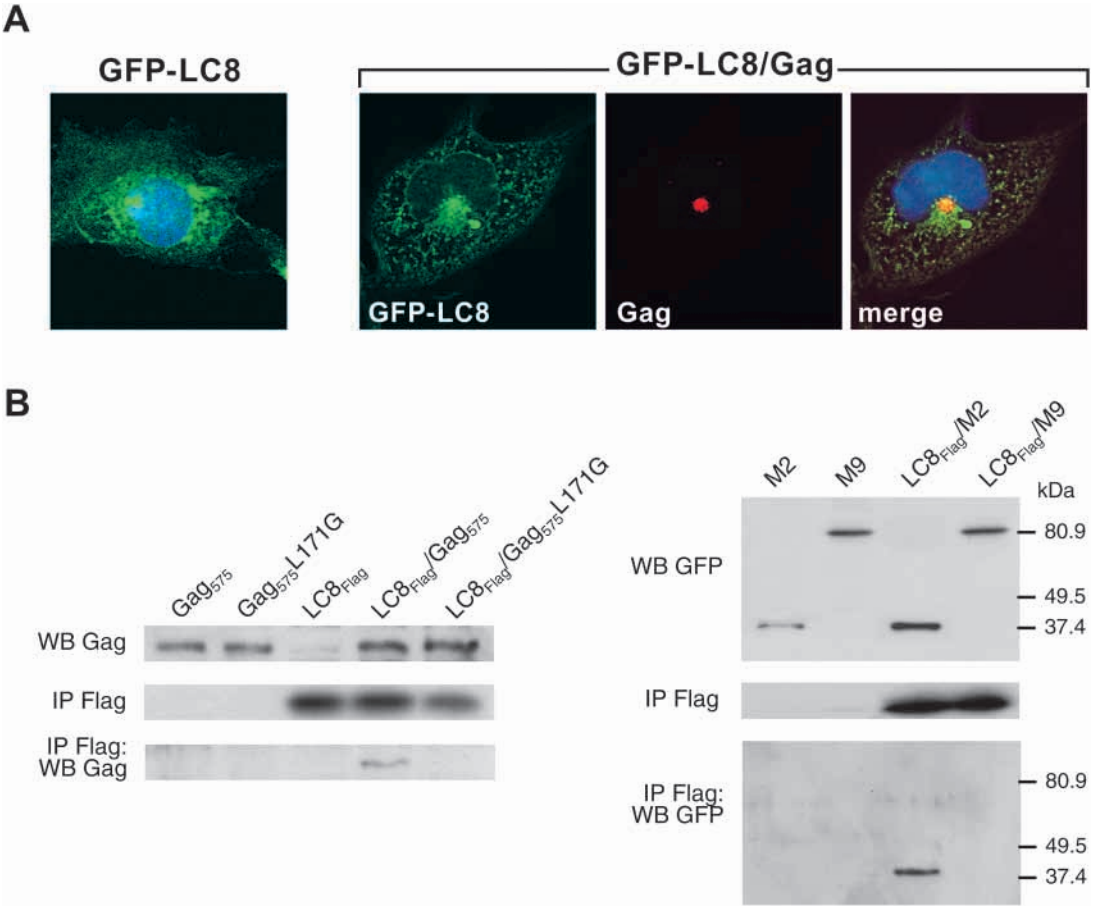

Fig. 5. Interaction between the structural Gag and the cytoplasmic light chain of dynein LC8. (A) Cos6 cells were co-transfected with pSG-Gag and pGFP-LC8, and analyzed 20 hours later. As shown in this confocal section, 97% of Gag co-localizes with GFP-LC8 at the MTOC [measured using Lasersharp software (BioRad)], whereas GFP-LC8 is evenly distributed in the cytoplasm when expressed alone. Nuclei are stained with DAPI. (B) A direct interaction between LC8 and Gag was observed by immunoprecipitation experiments followed by western blotting when 293T cells were co-transfected with the expression vectors, whereas the L171G mutation abolishes this interaction. Anti-Gag and anti-Flag antibodies do not precipitate LC8 or HFV Gag, respectively, when these proteins are expressed alone. A similar interaction was observed with the M2 mutant (GFP-Gag150-250) but not with the M9 mutant, which lacks the domain involved in MTOC targeting.

cells, whereas Gag was still associated with this organelle in cells transfected with empty DS-Red vector. These observations demonstrate that targeting of Gag to the MTOC requires the dynein-dynactin retrograde motor. In all these experiments, we only analysed cells that contained evenly distributed recombinant proteins, avoiding those (10% of the transfected cells) that harbored large protein aggregates already reported when using DsRed expressing vectors.

Finally, GFP-Gag transfected Cos6 cells were analysed by immunofluorescence following or not a treatment with nocodazole, 20 hours after transfection. As shown in Fig. 4B, Gag remains diffuse and punctate throughout the cytoplasm in treated cells, and is never detected at the MTOC under these settings. This observation suggests that the MT network is required to target the centrosome but also to stabilize Gag at the pericentrosomal region.

HFV Gag directly interacts with the cytoplasmic light chain of dynein

Cytoplasmic dynein is a large multisubunit motor complex that is composed of heavy, intermediate and light chains (Karki and Holzbaur, 1999). For lyssaviruses, a specific interaction has been demonstrated between the dynein light chain 8 (LC8) and the P phosphoprotein, a component of the viral ribonucleoprotein complex, providing a molecular basis for the axonal transport of these neurotropic viruses (Jacob et al., 2000; Raux et al., 2000). To assess whether HFV Gag could interact with LC8, we first examined their subcellular distribution in co-transfected cells. Confocal microscopy revealed that between 87% and 98% of Gag localized with GFP-LC8 at the MTOC, depending on the experiment analysed (Fig. 5A), consistent with a possible interaction between the molecules, whereas GFP-LC8 was distributed throughout the cytoplasm when expressed alone (Fig. 5A) (Alonso et al., 2001; Jacob et al., 2000).

To investigate this interaction further, co-immunoprecipitation experiments were performed following cell transfection. For this purpose, 293T cells were transfected with a vector encoding Gag, GagL171G or $LC8_{Flag}$, or with a combination of these vectors. A plasmid encoding the first 575 amino acids of Gag was used rather than the full-length

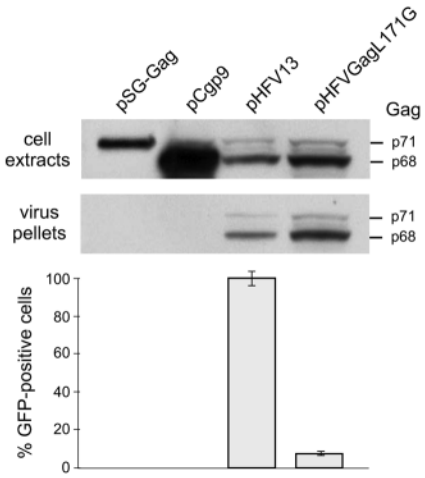

Fig. 6. Biological role of the coiled-coil motif. Western-blot analysis of cell extracts and virus pellets from cells transfected with the infectious clone pHFV13, the corresponding clone harboring the GagL171G mutation (pHFVGagL171G), pSG-Gag and pCgp9, detected by polyclonal anti-Gag antibodies. The virus titer from cells transfected with pHFV13, corresponding to 9×10^4 FCFU ml^{-1}, was arbitrarily set at 100%. The L171G point mutation does not affect particle release but dramatically reduces infectivity of the corresponding virus by more than 90% (6.2×10^3 FCFU ml^{-1}).

molecule because the full-length molecule is hardly immunoprecipitated by anti-Gag antibodies (Tobaly-Tapiero et al., 2001). Direct analysis of protein extracts from transfected cells using rabbit anti-Gag antibodies revealed the presence of Gag_{575} and the L171G mutant by western blot (Fig. 6B). By contrast, $LC8_{Flag}$ was detected by immunoprecipitation with anti-Flag antibodies in the corresponding transfected cells following metabolic labeling. These immune complexes were subsequently analysed by western blot using anti-Gag antibodies, revealing the presence of Gag_{575} in cells co-transfected with $pLC8_{Flag}$ and $pSG\text{-}Gag_{575}$, whereas no signal was detected in cells expressing Gag_{575}L171G and $LC8_{Flag}$ (Fig. 6B). Similarly, following the same procedure, an interaction with LC8 was detected when using the M2 mutant encoding GFP-Gag150-250, whereas no interaction was observed in cells co-transfected with a vector encoding GFP-Gag deleted from amino acids 144-277 (mutant M9), which lacks the domain required to target the MTOC.

These results demonstrate a direct interaction between the cytoplasmic light chain of dynein LC8 and the structural HFV Gag protein.

Effect of the GagL171G mutation on the viral cycle

Finally, to assess the biological role of the coiled-coil motif between amino acids 150 and 180 of HFV Gag in the virus cycle, a full-length viral clone harboring the L171G helix-breaking point mutation was constructed, and its behavior in tissue culture was compared with that of the parental infectious proviral clone. Cos6 were transfected with the wild-type pHFV13, pHFVGagL171G harboring the L171G mutation in the Gag ORF, pSG-Gag or pCgp9 (a vector encoding for only HFV Gag and Pol viral proteins); 72 hours later, viral protein expression in transfected cells and virus production in culture supernatants were evaluated. As shown in Fig. 7, in cell extracts both proviral clones express similar levels of Gag molecules, which are detected as a doublet of 71 kDa and 68 kDa by polyclonal anti-Gag antibodies, demonstrating that the L171G point mutation has no effect on Gag expression, stability and maturation. Indeed, the 71 kDa band corresponds to the full-length Gag precursor (p71), as visualized in pSG-Gag transfected cells, whereas the 68 kDa product represents its main cleavage product (p68), mirroring the presence of an active viral protease (Giron et al., 1997). To assess whether the Gag mutation affected virus egress, supernatants from transfected cells were ultracentrifuged on a sucrose gradient and the resulting pellets, which contained extracellular virions were analysed by western blot using polyclonal anti-Gag antibodies. In that case, no major difference was observed between pHFV13 and pHFVGagL171G, demonstrating that virus egress was not impaired by this helix-breaking point mutation in Gag. No viral particles were produced from neither pSG-Gag- or pCgp9-transfected cells as expected because, in contrast to other retroviruses, FV particle formation requires the presence of the homologous envelope (Pietschmann et al., 1999).

Finally, virus production in culture supernatants was evaluated following infection of an indicator cell line (the FAG cells), which harbor the GFP ORF under the control of the HFV LTR as already described (Tobaly-Tapiero et al., 2001). Direct fluorescence observed 48 hours after infection reveals a significant virus production from pHFV13 transfected cells (9×10^4 FCFU ml^{-1}), whereas the Gag mutation dramatically reduced infectivity of the corresponding provirus but did not totally abolished it (6.2×10^3 FCFU ml^{-1}). Values are averages of three independent experiments.

Altogether, our data demonstrate that the L171G mutation in the Gag ORF has no effect on virus egress but drastically reduces infectivity of the corresponding proviral clone.

Discussion

Several bacteria and viruses have been shown to subvert the cytoskeleton for their intracellular trafficking (Dramsi and Cossart, 1998; Frischknecht and Way, 2001; Ploubidou and Way, 2001; Sodeik, 2000). However, despite a growing body of knowledge accumulating in this field, how retroviruses reach the nucleus of the newly infected cell is still poorly understood. To shed a new light on this stage of viral replication, we have studied the route taken by HFV, an animal retrovirus, during the early steps of infection.

By EM, we show here that incoming HFV proteins concentrate in the pericentrosomal region as free and structured capsids close to MTs. More viral capsids surround the MTOC than expected from the multiplicity of infection used. Indeed, most extracellular retroviral particles produced during an infection harbor a defective genome and are therefore unable to transactivate the viral LTR of GFP-indicator cells (Tobaly-Tapiero et al., 2001). In the case of HIV-1, it has been reported that infectivity to particle ratio is as low as 1 in 60,000 (Kimpton and Emerman, 1992; Piatak et al., 1993), whereas a more recent study softened this conclusion by showing a ratio up to 1 infectious particle in 10 (Andreadis et al., 2000). Furthermore, we demonstrate that the determinants required to reach the pericentrosomal area are harbored by the scaffold component of viral capsids, the structural Gag protein, because

this protein alone targets the centrosome in transfected cells in the absence of other viral partners.

Because the vimentin network is not affected in Gag-transfected cells, accumulation of Gag around the MTOC does not trigger the formation of an aggresome. However, similar to the formation of this inclusion body (Garcia-Mata et al., 1999), Gag transport towards the MTOC involves the retrograde dynein-dynactin motor, because it is prevented by overproduction of CC1, the central coiled-coil domain of $p150^{Glued}$, reported to disrupt the function of this retrograde motor. Other viruses have been shown to use the MT network for their intracellular transport. For instance, adenovirus type 2 (Ad2) and HSV, two nuclear replicative DNA viruses entering the cell through receptor-mediated endocytosis and direct membrane fusion respectively, are transported as naked capsids towards the nucleus via the MT network (Sodeik et al., 1997; Soll, 1997). For ASFV and rabies viruses, two other viruses that use the MT network to move within the infected cell, an interaction with LC8 forms a molecular basis of this trafficking (Alonso et al., 2001; Jacob et al., 2000; Raux et al., 2000). The interaction between LC8 and HFV Gag described here could play such a role in the case of FVs.

LC8 was first identified as an integral component of the *Chlamydomonas reinhardtii* outer dynein arm (Pfister et al., 1982; Piperno and Luck, 1979). Since then, this evolutionarily conserved molecule has been shown to interact with many cellular complexes, such as the nitric oxide synthase (Jaffrey and Snyder, 1996) and myosin V (Goode et al., 2000; Naisbitt et al., 2000), an actin-based motor mainly located at the plasma membrane that shuttles between the cell periphery and the MTOC along the MT network (Espreafico et al., 1998; Tsakraklides et al., 1999). LC8 is encoded by at least two genes in humans (Naisbitt et al., 2000), leading to the synthesis of dynein light chain 2 (DLC2) and dynein light chain 1 (DLC1), the isoform used in our work. Interestingly, myosin V has been shown to interact with DLC2 but not with DLC1 (Naisbitt et al., 2000; Puthalakath et al., 2001). Thus, migration of HFV capsids towards the centrosome on the microtubule network probably involves an interaction with dynein LC8 (DLC1) rather than myosin V LC8 (DLC2). In that sense, HFV efficiently targets the centrosomal region and replicates in myosin-V-deficient melanoma S91-6 cells (E. Espreafico and A. Saïb, unpublished). However, we cannot exclude the possibility that HFV Gag also interacts with DLC2 as a component of myosin V, favoring its trafficking on actin beneath the plasma membrane devoid of microtubules. Therefore, interaction between incoming FV capsids and the multifunctional LC8 could provide a bridge to shuttle between an actin-based motor beneath the plasma membrane and the MT network within the cytoplasm. Remarkably, a similar MT- and dynein-dependent trafficking towards the centrosome was recently described for incoming HIV-1, although the viral and cellular protagonists involved in this retrograde transport were not determined (McDonald et al., 2002). Nevertheless, these observations suggest that distinct classes of retroviruses might tether the dynein-dynactin complex motor on the MT network during the early stage of infection to reach the nucleus, opening new perspectives in the development of anti-retroviral drugs.

Analysis of the subcellular distribution of Gag deletion mutants reveals that the GR boxes as well as the determinants involved in capsid assembly (the Gag-Gag interaction domain and the CTRS) are not required to target the centrosome, whereas amino acids 150-180 are necessary to reach this organelle. This region does not harbor any obvious similarities with the two previously described LC8-interacting motifs, (K/R)XTQT and GIQVD (Lo et al., 2001; Rodriguez-Crespo et al., 2001), but a coiled-coil motif conserved in all primate foamy viruses (Tobaly-Tapiero et al., 2001) seems to be involved in centriolar targeting of Gag. In that sense, a single point mutation (L171G) in the Gag ORF, leading to the disruption of the coiled-coil motif, abolishes MTOC targeting of the corresponding GFP-Gag fusion and renders a full-length viral clone non-infectious. Indeed, whereas Gag assembly and virus release are not affected by this helix-breaking point mutation, productive infection of naive cells is dramatically reduced. Because this mutation was shown to prevent Gag/LC8 interaction, tethering of the dynein retrograde motor following its entry into the cytoplasm might be impaired, a hypothesis that we are currently exploring. The L171G point mutation does not totally abolish infectivity, suggesting that other trafficking pathways might be used by FVs to reach the center of the cell. In that sense, intracellular trafficking involving the actin cytoskeleton might account for this observation, an alternative route already put forward for HIV-1 (McDonald et al., 2002) and previously suggested for FVs because Gag was also shown to interact with actin (Giron et al., 1997).

HFV Gag is not the unique partner of LC8 lacking the two characterized LC8-interacting motifs. Interestingly, all these proteins harbor an α-helical coiled-coil in the domain identified as the LC8-binding region. For example, the LC8-interacting domain of myosin V is predicted to fold into an amphiphilic helix (Naisbitt et al., 2000) and, similarly, the signal response domain of IκBα, which was shown to interact with LC8 (Crepieux et al., 1997), folds into a coiled coil as revealed by the COILS program (data not shown). Such a hypothesis might also apply to the neuronal form of nitric oxide synthase (nNOS) (Benashski et al., 1997). Given that LC8 harbors a similar amphiphilic helix triggering its multimerization (Benashski et al., 1997), interactions between LC8 and myosin V, IκBα, nNOS and HFV Gag might occur via such specific protein motif interface, constituting a new mode of contact with LC8.

One remaining issue is how the viral genome, wrapped by Gag molecules, is imported into the nucleus. Interestingly, the dynein-dynactin complex has recently been shown to associate with the nuclear envelope, facilitating the remodeling of this physical frontier (Busson et al., 1998; Salina et al., 2002). Therefore, interaction of Gag with the dynein-dynactin complex could not only drive incoming viral capsids towards the centrosome but also be involved in their subsequent targeting to the nuclear envelope. Yet, HFV capsids were never detected within the nucleus, nor close to nuclear pores, even later during the replication cycle [here and Fischer et al. (Fischer et al., 1998)], whereas unassembled Gag proteins and the viral genome are detected in the nucleus early after infection (Saib et al., 1997; Schliephake and Rethwilm, 1994). Therefore, in contrast to Ad2 or HSV, those capsids dock to the nuclear pore triggering nuclear translocation of the viral genome (Greber et al., 1997; Ojala et al., 2000; Trotman et al., 2001), nuclear import of HFV Gag and genome must be accompanied by disassembly or significant deformation of the core particle at the MTOC.

We thank T. Schroer for providing the p50/dynamitin and DsRed-CC1 vectors, E. Espreafico for providing S91-6 melanoma cells, M. Bornens for providing anti-centriole antibodies, F. Puvion for EM pictures, C.-H. Lecellier and A. Saumet for their help, the LPH and F. Brau for the photographic work, and F. Perez, C. Pique and V. Lallemand for critical reading of the manuscript and for their kind help. This study was supported by ARC (grant #5981) and F. Lacoste. CP is supported by SIDACTION/Ensemble Contre le Sida (grant #AO12-2).

References

Alonso, C., Miskin, J., Hernaez, B., Fernandez-Zapatero, P., Soto, L., Canto, C., Rodriguez-Crespo, I., Dixon, L. and Escribano, J. M. (2001). African swine fever virus protein p54 interacts with the microtubular motor complex through direct binding to light-chain dynein. *J. Virol*. **75**, 9819-9827.

Andreadis, S., Lavery, T., Davis, H. E., Le Doux, J. M., Yarmush, M. L. and Morgan, J. R. (2000). Toward a more accurate quantitation of the activity of recombinant retroviruses: alternatives to titer and multiplicity of infection. *J. Virol*. **74**, 1258-1266.

Benashski, S. E., Harrison, A., Patel-King, R. S. and King, S. M. (1997). Dimerization of the highly conserved light chain shared by dynein and myosin V. *J. Biol. Chem*. **272**, 20929-20935.

Burkhardt, J. K., Echeverri, C. J., Nilsson, T. and Vallee, R. B. (1997). Overexpression of the dynamitin (p50) subunit of the dynactin complex disrupts dynein-dependent maintenance of membrane organelle distribution. *J. Cell Biol.* **139**, 469-484.

Busson, S., Dujardin, D., Moreau, A., Dompierre, J. and De Mey, J. R. (1998). Dynein and dynactin are localized to astral microtubules and at cortical sites in mitotic epithelial cells. *Curr. Biol.* **8**, 541-544.

Crepieux, P., Kwon, H., Leclerc, N., Spencer, W., Richard, S., Lin, R. and Hiscott, J. (1997). I kappa B alpha physically interacts with a cytoskeleton-associated protein through its signal response domain. *Mol. Cell. Biol*. **17**, 7375-7385.

Dohner, K., Wolfstein, A., Prank, U., Echeverri, C., Dujardin, D., Vallee, R. and Sodeik, B. (2002). Function of dynein and dynactin in herpes simplex virus capsid transport. *Mol. Biol. Cell*. **13**, 2795-2809.

Dramsi, S. and Cossart, P. (1998). Intracellular pathogens and the actin cytoskeleton. *Annu. Rev. Cell. Dev. Biol*. **14**, 137-166.

Eastman, S. W. and Linial, M. L. (2001). Identification of a conserved residue of foamy virus Gag required for intracellular capsid assembly. *J. Virol*. **75**, 6857-6864.

Espreafico, E. M., Coling, D. E., Tsakraklides, V., Krogh, K., Wolenski, J. S., Kalinec, G. and Kachar, B. (1998). Localization of myosin-V in the centrosome. *Proc. Natl. Acad. Sci. USA* **95**, 8636-8641.

Fischer, N., Heinkelein, M., Lindemann, D., Enssle, J., Baum, C., Werder, E., Zentgraf, H., Muller, J. G. and Rethwilm, A. (1998). Foamy virus particle formation. *J. Virol*. **72**, 1610-1615.

Frischknecht, F. and Way, M. (2001). Surfing pathogens and the lessons learned for actin polymerization. *Trends Cell Biol*. **11**, 30-38.

Frischknecht, F., Moreau, V., Rottger, S., Gonfloni, S., Reckmann, I., Superti-Furga, G. and Way, M. (1999). Actin-based motility of vaccinia virus mimics receptor tyrosine kinase signalling. *Nature* **401**, 926-929.

Garcia-Mata, R., Bebok, Z., Sorscher, E. J. and Sztul, E. S. (1999). Characterization and dynamics of aggresome formation by a cytosolic GFP-chimera. *J. Cell Biol.* **146**, 1239-1254.

Geada, M. M., Galindo, I., Lorenzo, M. M., Perdiguero, B. and Blasco, R. (2001). Movements of vaccinia virus intracellular enveloped virions with GFP tagged to the F13L envelope protein. *J. Gen. Virol*. **82**, 2747-2760.

Giron, M. L., Colas, S., Wybier, J., Rozain, F. and Emanoil-Ravier, R. (1997). Expression and maturation of human foamy virus Gag precursor polypeptides. *J. Virol*. **71**, 1635-1639.

Goode, B. L., Drubin, D. G. and Barnes, G. (2000). Functional cooperation between the microtubule and actin cytoskeletons. *Curr. Opin. Cell Biol.* **12**, 63-71.

Greber, U. F., Suomalainen, M., Stidwill, R. P., Boucke, K., Ebersold, M. W. and Helenius, A. (1997). The role of the nuclear pore complex in adenovirus DNA entry. *EMBO J.* **16**, 5998-6007.

Heath, C. M., Windsor, M. and Wileman, T. (2001). Aggresomes resemble sites specialized for virus assembly. *J. Cell Biol.* **153**, 449-455.

Hollinshead, M., Rodger, G., Van Eijl, H., Law, M., Hollinshead, R., Vaux, D. J. and Smith, G. L. (2001). Vaccinia virus utilizes microtubules for movement to the cell surface. *J. Cell Biol.* **154**, 389-402.

Jacob, Y., Badrane, H., Ceccaldi, P. E. and Tordo, N. (2000). Cytoplasmic dynein LC8 interacts with lyssavirus phosphoprotein. *J. Virol*. **74**, 10217-10222.

Jaffrey, S. R. and Snyder, S. H. (1996). PIN: an associated protein inhibitor of neuronal nitric oxide synthase. *Science* **274**, 774-777.

Johnston, J. A., Ward, C. L. and Kopito, R. R. (1998). Aggresomes: a cellular response to misfolded proteins. *J. Cell Biol.* **143**, 1883-1898.

Karki, S. and Holzbaur, E. L. (1999). Cytoplasmic dynein and dynactin in cell division and intracellular transport. *Curr. Opin. Cell. Biol*. **11**, 45-53.

Kimpton, J. and Emerman, M. (1992). Detection of replication-competent and pseudotyped human immunodeficiency virus with a sensitive cell line on the basis of activation of an integrated beta-galactosidase gene. *J. Virol*. **66**, 2232-2239.

Kopito, R. R. (2000). Aggresomes, inclusion bodies and protein aggregation. *Trends Cell Biol*. **10**, 524-530.

Lo, K. W., Naisbitt, S., Fan, J. S., Sheng, M. and Zhang, M. (2001). The 8-kDa dynein light chain binds to its targets via a conserved (K/R)XTQT motif. *J. Biol. Chem*. **276**, 14059-14066.

McDonald, D., Vodicka, M. A., Lucero, G., Svitkina, T. M., Borisy, G. G., Emerman, M. and Hope, T. J. (2002). Visualization of the intracellular behavior of HIV in living cells. *J. Cell Biol.* **159**, 441-452.

Moreau, V., Frischknecht, F., Reckmann, I., Vincentelli, R., Rabut, G., Stewart, D. and Way, M. (2000). A complex of N-WASP and WIP integrates signalling cascades that lead to actin polymerization. *Nat. Cell Biol*. **2**, 441-448.

Naisbitt, S., Valtschanoff, J., Allison, D. W., Sala, C., Kim, E., Craig, A. M., Weinberg, R. J. and Sheng, M. (2000). Interaction of the postsynaptic density-95/guanylate kinase domain-associated protein complex with a light chain of myosin-V and dynein. *J. Neurosci*. **20**, 4524-4534.

Ojala, P. M., Sodeik, B., Ebersold, M. W., Kutay, U. and Helenius, A. (2000). Herpes simplex virus type 1 entry into host cells: reconstitution of capsid binding and uncoating at the nuclear pore complex in vitro. *Mol. Cell. Biol*. **20**, 4922-4931.

Pfister, K. K., Fay, R. B. and Witman, G. B. (1982). Purification and polypeptide composition of dynein ATPases from *Chlamydomonas* flagella. *Cell Motil.* **2**, 525-547.

Piatak, M., Saag, M. S., Yang, L. C., Clark, S. J., Kappes, J. C., Luk, K. C., Hahn, B. H., Shaw, G. M. and Lifson, J. D. (1993). High levels of HIV-1 in plasma during all stages of infection determined by competitive PCR. *Science* **259**, 1749-1754.

Pietschmann, T., Heinkelein, M., Heldmann, M., Zentgraf, H., Rethwilm, A. and Lindemann, D. (1999). Foamy virus capsids require the cognate envelope protein for particle export. *J. Virol*. **73**, 2613-2621.

Piperno, G. and Luck, D. J. (1979). Axonemal adenosine triphosphatases from flagella of *Chlamydomonas reinhardtii*. Purification of two dyneins. *J. Biol. Chem*. **254**, 3084-3090.

Ploubidou, A. and Way, M. (2001). Viral transport and the cytoskeleton. *Curr. Opin. Cell Biol.* **13**, 97-105.

Ploubidou, A., Moreau, V., Ashman, K., Reckmann, I., Gonzalez, C. and Way, M. (2000). Vaccinia virus infection disrupts microtubule organization and centrosome function. *EMBO J.* **19**, 3932-3944.

Puthalakath, H., Villunger, A., O'Reilly, L. A., Beaumont, J. G., Coultas, L., Cheney, R. E., Huang, D. C. and Strasser, A. (2001). Bmf: a proapoptotic BH3-only protein regulated by interaction with the myosin V actin motor complex, activated by anoikis. *Science* **293**, 1829-1832.

Quintyne, N. J., Gill, S. R., Eckley, D. M., Crego, C. L., Compton, D. A. and Schroer, T. A. (1999). Dynactin is required for microtubule anchoring at centrosomes. *J. Cell Biol.* **147**, 321-334.

Raux, H., Flamand, A. and Blondel, D. (2000). Interaction of the rabies virus P protein with the LC8 dynein light chain. *J. Virol*. **74**, 10212-10216.

Rietdorf, J., Ploubidou, A., Reckmann, I., Holmstrom, A., Frischknecht, F., Zettl, M., Zimmermann, T. and Way, M. (2001). Kinesin-dependent movement on microtubules precedes actin-based motility of vaccinia virus. *Nat. Cell Biol*. **3**, 992-1000.

Rodriguez-Crespo, I., Yelamos, B., Roncal, F., Albar, J. P., Ortiz de Montellano, P. R. and Gavilanes, F. (2001). Identification of novel cellular proteins that bind to the LC8 dynein light chain using a pepscan technique. *FEBS Lett.* **503**, 135-141.

Saib, A., Puvion-Dutilleul, F., Schmid, M., Peries, J. and de The, H. (1997). Nuclear targeting of incoming human foamy virus Gag proteins involves a centriolar step. *J. Virol*. **71**, 1155-1161.

Salina, D., Bodoor, K., Eckley, M. D., Schroer, T. A., Rattner, J. B. and Burke, B. (2002). Cytoplasmic dynein as a facilitator of nuclear envelope breakdown. *Cell* **108**, 97-107.

Schliephake, A. W. and Rethwilm, A. (1994). Nuclear localization of foamy virus Gag precursor protein. *J. Virol*. **68**, 4946-4954.

Sodeik, B. (2000). Mechanisms of viral transport in the cytoplasm. *Trends Microbiol*. **8**, 465-472.

Sodeik, B., Ebersold, M. W. and Helenius, A. (1997). Microtubule-mediated transport of incoming herpes simplex virus 1 capsids to the nucleus. *J. Cell Biol.* **136**, 1007-1021.

Soll, D. R. (1997). Researchers in cell motility and the cytoskeleton can play major roles in understanding AIDS. *Cell Motil. Cytoskeleton* **37**, 91-97.

Suomalainen, M., Nakano, M. Y., Keller, S., Boucke, K., Stidwill, R. P. and Greber, U. F. (1999). Microtubule-dependent plus- and minus end-directed motilities are competing processes for nuclear targeting of adenovirus. *J. Cell Biol.* **144**, 657-672.

Tang, Y., Winkler, U., Freed, E. O., Torrey, T. A., Kim, W., Li, H., Goff, S. P. and Morse, H. C., 3rd (1999). Cellular motor protein KIF-4 associates with retroviral Gag. *J. Virol*. **73**, 10508-10513.

Tobaly-Tapiero, J., Bittoun, P., Giron, M. L., Neves, M., Koken, M., de The, H. and Saib, A. (2001). Human foamy virus capsid formation requires an interaction domain in the N terminus of Gag. *J. Virol*. **75**, 4367-4375.

Trotman, L. C., Mosberger, N., Fornerod, M., Stidwill, R. P. and Greber, U. F. (2001). Import of adenovirus DNA involves the nuclear pore complex receptor CAN/Nup214 and histone H1. *Nat. Cell Biol*. **3**, 1092-1100.

Tsakraklides, V., Krogh, K., Wang, L., Bizario, J. C., Larson, R. E., Espreafico, E. M. and Wolenski, J. S. (1999). Subcellular localization of GFP-myosin-V in live mouse melanocytes. *J. Cell Sci.* **112**, 2853-2865.

Ward, B. M. and Moss, B. (2001). Vaccinia virus intracellular movement is associated with microtubules and independent of actin tails. *J. Virol*. **75**, 11651-11663.

Yu, S. F., Edelmann, K., Strong, R. K., Moebes, A., Rethwilm, A. and Linial, M. L. (1996). The carboxyl terminus of the human foamy virus Gag protein contains separable nucleic acid binding and nuclear transport domains. *J. Virol*. **70**, 8255-8262.